DOI: 10.1002/cmdc.200700014

Nonphosphate Inhibitors of IspE Protein, a Kinase in the Non-Mevalonate Pathway for Isoprenoid Biosynthesis and a Potential Target for Antimalarial Therapy

Anna K. H. Hirsch,[a] Susan Lauw,[b] Philipp Gersbach,[a] W. Bernd Schweizer,[a] Felix Rohdich,[b] Wolfgang Eisenreich,*[b] Adelbert Bacher,[b] and François Diederich*[a]

The discovery of the non-mevalonate pathway for the biosynthesis of the isoprenoid precursors isopentenyl diphosphate (IPP, **1**) and dimethylallyl diphosphate (DMAPP, **2**) in the 1990s opened the way for new approaches in the fight against infectious diseases. This pathway starts with the condensation of pyruvate **3** and glyceraldehyde 3-phosphate **4** and is used exclusively by pathogenic bacteria such as *Mycobacterium tuberculosis*, and by the protozoan *Plasmodium* parasites (Scheme 1).[1] Mammals, on the other hand, use the alternative mevalonate pathway. Hence, the development of small-molecule inhibitors for the enzymes of the non-mevalonate pathway constitutes a novel approach in the treatment of important infectious diseases.[2]

Malaria is without a doubt the most important and devastating tropical disease with 300–500 million clinical cases and between one and three million deaths a year. In light of the emergence of drug and insecticide resistance, the need for medicines with a novel mode of action is ever increasing.[3]

Inhibition of the enzymes of the non-mevalonate pathway by low-molecular-weight ligands constitutes a true challenge. The active sites for complexation and transformation of their phosphate- and diphosphate-based substrates are highly polar and do not offer much concave hydrophobic surface. Correspondingly, most of the few inhibitors known today are phosphates or phosphonates,[2,4–6] such as the best-known example, *Fosmidomycin*,[2a,5] which binds to IspC (1-deoxy-D-xylulose 5-phosphate reductoisomerase, EC 1.1.1.267) and is currently in clinical trials.

We selected the kinase IspE (4-diphosphocytidyl-2*C*-methyl-D-erythritol (CDP-ME) kinase, EC 2.7.1.148) in the center of the non-mevalonate pathway as a target for structure-based inhibitor design.[7] IspE catalyzes the phosphorylation of the 2-OH group of 4-diphosphocytidyl-2*C*-methyl-D-erythritol (**5**) forming 4-diphosphocytidyl-2*C*-methyl-D-erythritol-2-phosphate (**6**) (Scheme 1).[8] Two X-ray crystal structures have been published; the apoenzyme of *Thermus thermophilus* (1.7 Å resolution, Protein Data Bank (PDB) code: 1UEK)[9a] and a ternary complex of *Escherichia coli* (2.0 Å resolution, PDB code: 1OJ4) with bound CDP-ME and a nonhydrolyzable ATP analogue, 5′-adenyl-β,γ-amidotriphosphate (AppNp).[9b] Herein, we report the first inhibitors of IspE (compounds (±)-**7**, **8**–**10**, (±)-**11**–(±)-**17**, and **18** (Figure 1)) with competitive inhibition constants (K_{ic}) in the upper nanomolar range. They feature two salient characteristics: they are drug-like and do not contain any phosphate or phosphonate residues. Also, in contrast to most reported kinase inhibitors,[6] they do not occupy the adenine binding site.

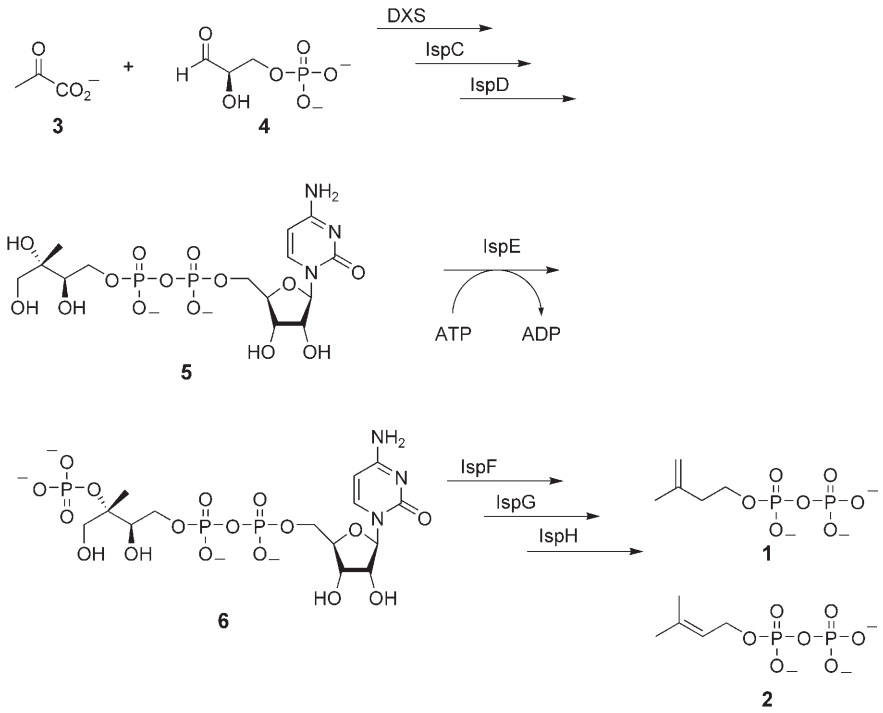

Scheme 1. The non-mevalonate pathway for the biosynthesis of the isoprenoid precursors IPP **1** and DMAPP **2**.[1] DXS = 1-deoxy-D-xylulose 5-phosphate synthase, ATP = adenosine triphosphate, ADP = adenosine diphosphate.

[a] *A. K. H. Hirsch, P. Gersbach, Dr. W. B. Schweizer, Prof. Dr. F. Diederich*
Laboratorium für Organische Chemie, ETH Zürich, Hönggerberg, HCI, 8093 Zürich (Switzerland)
Fax: (+41) 44-632-1109
E-mail: diederich@org.chem.ethz.ch

[b] *S. Lauw, Dr. F. Rohdich, Dr. W. Eisenreich, Prof. Dr. A. Bacher*
Lehrstuhl für Organische Chemie und Biochemie, Technische Universität München, Lichtenbergstrasse 4, 85748 Garching (Germany)
Fax: (+49) 89-289-13363

Supporting information for this article is available on the WWW under http://www.chemmedchem.org or from the author.

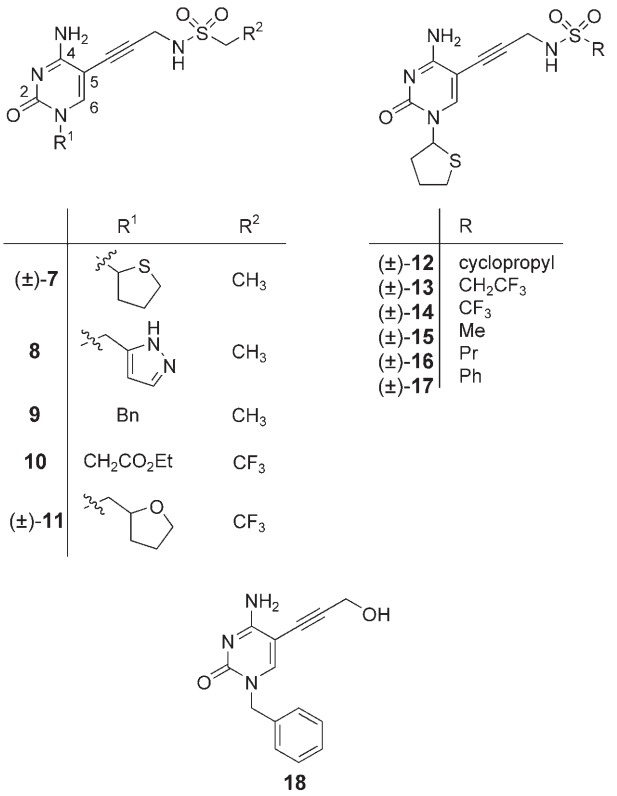

	R^1	R^2
(±)-**7**		CH_3
8		CH_3
9	Bn	CH_3
10	CH_2CO_2Et	CF_3
(±)-**11**		CF_3

	R
(±)-**12**	cyclopropyl
(±)-**13**	CH_2CF_3
(±)-**14**	CF_3
(±)-**15**	Me
(±)-**16**	Pr
(±)-**17**	Ph

Figure 1. Potential inhibitors of IspE.

For our design purposes, we chose the X-ray crystal structure of the ternary complex[9b] which shows IspE to be a homodimer with two active sites at either end of a solvent-filled tunnel (Figure 2).

Each active site features three pockets: the adenosine, the cytidine, and the ME/phosphate pockets. Molecular modeling analysis using the program MOLOC[10] revealed that the cytidine binding site has an additional small, hydrophobic pocket associated with it (Figure 3 and Figure 1SI (Supporting Informa-

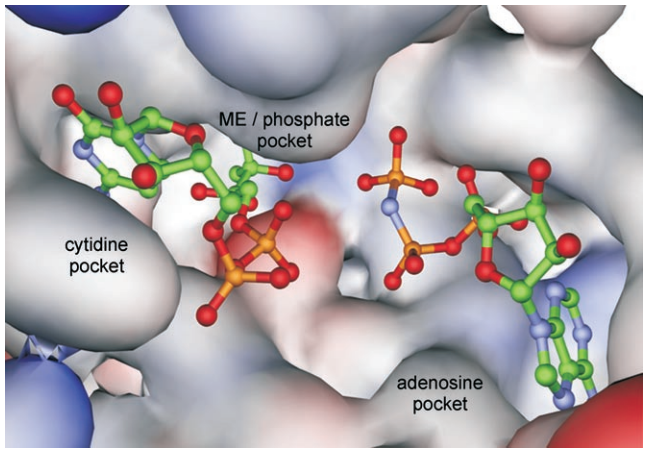

Figure 2. Active site of IspE as revealed in the ternary complex with CDP-ME and a nonhydrolizable ATP analogue, 5′-adenyl-β,γ-amidotriphosphate (AppNp) (PDB code: 1J4).[9b] The two nucleotides bind on opposite sites of the solvent-filled channel that hosts the phosphate moieties. Color code: see caption to Figure 3.

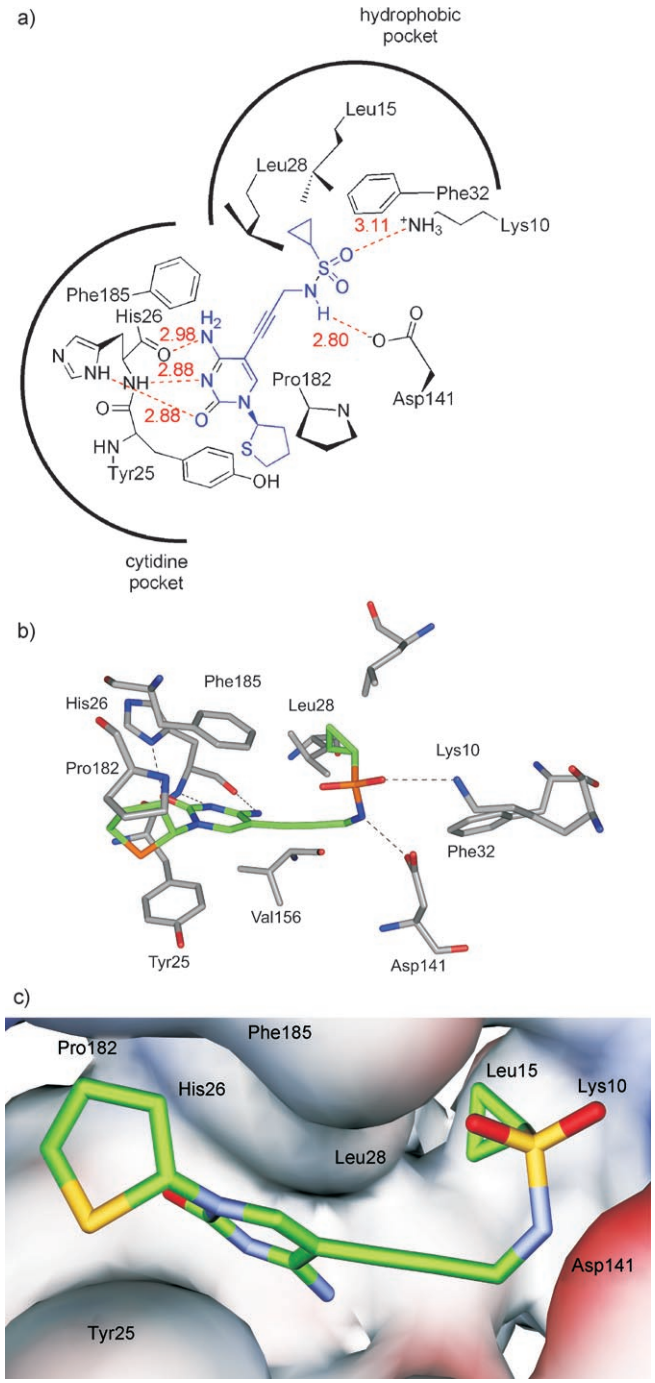

Figure 3. a) Schematic representation of the binding mode of the representative inhibitor (±)-**12** (in blue) with potential H-bonds depicted as red dashed lines as predicted by modeling. Distances between heavy atoms are given in Å. b) Computer model of the proposed binding mode of (*R*)-**12**. A similar binding mode is predicted for the (*S*)-enantiomer. Dashed lines are shown for H-bonding contacts below 3.1 Å (distances between heavy atoms). For the modeling, the following applies throughout the article, if not otherwise stated: the unchanged coordinates of IspE (PDB code: 1OJ4) were used; only the geometry of the bound ligand was optimized during the simulation. In these geometry optimizations, the staggered conformation of the sulfonamide moiety was fixed, with a dihedral angle C(sp^3)-*N*-S-C-(sp^3) of approximately −60°. Color code: ligand skeleton: green; C: gray; O: red; N: blue; S: yellow. This distance selection for H-bonding and the color code are maintained throughout the article, if not otherwise stated. c) Proposed binding of inhibitor (±)-**12** in the hydrophobic subpocket lined by Leu 15, Leu 28, and Phe 185.

tion)). This pocket, lined by Leu 15, Leu 28, and Phe 185, could possibly be important for feedback regulation of IspE by downstream products of the biosynthetic pathway. A superposition of the two published X-ray crystal structures (Figure 1SI) and sequence alignments (Figure 2SI) clearly show that this subpocket is well conserved amongst different organisms. Our first-generation inhibitors (Figure 1) were designed to occupy both the cytidine and this hydrophobic subpocket (Figure 3 b),[6] leaving the hydrophilic ME/phosphate and the adenosine pocket unoccupied.

On the way towards a first series of active inhibitors, we decided to maintain cytosine as a central scaffold. The design strategy is illustrated for ligand (±)-**12** in Figure 3. The nucleobase is sandwiched between Tyr 25 and Phe 185 (Figure 3 b). Similar to the natural substrate CDP-ME, the cytosine moiety is postulated to undergo H-bonding to both backbone and side chain of His 26 ($d(O_{His}\cdots N) = 2.98$ Å, $d(N_{His}\cdots N) = 2.88$ Å, and $d(N_{His}\cdots O) = 2.88$ Å). As ribose analogues, we selected a number of heteroalicyclic (such as a tetrahydrothiophenyl ring in (±)-**12**) and aromatic rings to fill the space of a pseudo-sandwich made of Pro 182 and Tyr 25. Modeling predicts that both enantiomers of the tetrahydrothiophenyl and tetrahydrofuranyl derivates should bind with similar strength because of the conformational flexibility (puckering) of the five-membered rings. To reach into the small hydrophobic subpocket, a propargylic sulfonamide linker departing from C5 of the cytosine scaffold seemed most suitable, with the triple bond ensuring a certain rigidity and linearity of the vector. The sulfonamide moiety was expected to undergo ionic H-bonding with the side chain of Asp 141 ($d(N\cdots O_{Asp}) = 2.80$ Å) and the side chain of Lys 10 ($d(S\cdots N_{Lys}) = 3.11$ Å). Furthermore, in the preferred conformation of N-substituted sulfonamides, the lone pair of the N-atom bisects the O-S-O angle, resulting in a staggered arrangement.[11] In this conformation, small complementary residues, such as the cyclopropyl group in (±)-**12**, orient directly into the tight, hydrophobic pocket lined by Leu 15, Leu 28, and Phe 185.

The synthesis of the representative target molecule (±)-**12** is shown in Scheme 2 (for the synthesis and characterization of the other new ligands, see the Supporting Information). Reaction of propargyl amine (**19**) with sulfonyl chloride **20** provided the propargylic sulfonamide **21**. Regiospecific iodination of cytosine (**22**) yielded 5-iodocytosine (**23**),[12] which was converted in a Pummerer-like reaction with tetramethylene sulfoxide (**24**) to the tetrahydrothiophenyl derivative **25**.[13] Sonogashira cross-coupling of alkyne **21** and cytosine derivative (±)-**25** afforded the target compound (±)-**12** in excellent yield.

An X-ray crystal structure of the 2,2,2-trifluoroethyl derivative (±)-**13** was obtained (Figure 4), which nicely supported the preference of the sulfonamide residue for the staggered conformation, with the N-lone pair bisecting the O-S-O angle. The observed conformation (see the caption to Figure 4 for relevant dihedral angles), with the trifluoroethyl residue folded back towards the nucleobase, can be rationalized by a more favorable, denser crystal packing.

The IC_{50} (IC_{50} = concentration of inhibitor at which 50% maximal initial velocity is observed) and K_i values were determined using an enzyme-coupled photometric assay (Table 1 and Supporting Information).[14] The mode of inhibition was assigned using the program Dynafit.[15] The inhibition was verified for selected ligands with a direct NMR spectroscopic assay. This assay monitors the consumption of ^{13}C-labeled substrate and the concomitant formation of product (for exemplary K_i and IC_{50} curves, see Figure 3SI and Figure 4SI).[14]

The biological assays demonstrate potent inhibition of IspE protein, with K_{ic} (competitive inhibition constant) values of the

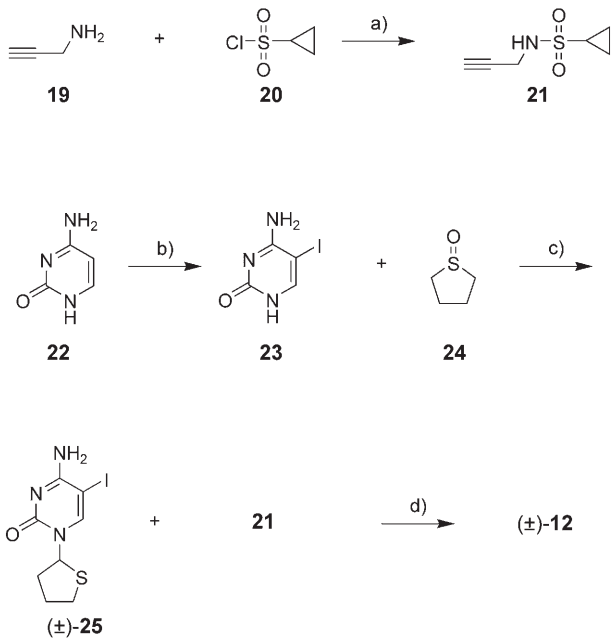

Scheme 2. Synthesis of inhibitor (±)-**12**. a) Et_3N, CH_2Cl_2, 25 °C, 5 min, 72%; b) I_2, HIO_3, AcOH, CCl_4, H_2O, 50 °C, 16 h, 85%; c) TMSOTf, Et_3N, ZnI_2, toluene, 0 °C→25 °C, 17 h, 60%; d) Et_3N, $[PdCl_2(PPh_3)_2]$, CuI, DMF, 25 °C, 22 h, 94%. TMSOTf = Trimethylsilyl trifluoromethanesulfonate, DMF = *N*,*N*-dimethylformamide.

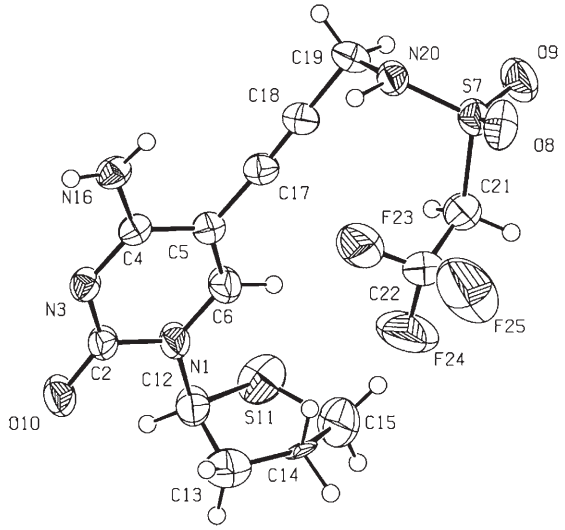

Figure 4. Ortep plot of the X-ray crystal structure of inhibitor (±)-**13** at 223 K with arbitrary numbering scheme. Thermal ellipsoids of the non-H-atoms are shown at the 50% probability level. Selected dihedral angles: C(17)-C(18)-C(19)-N(20) = 16°; C(18)-C(19)-N(20)-S(7) = 90°; C(19)-N(20)-S(7)-C(21) = −68°.

Table 1.
Biological activities and Clog*P* values of IspE inhibitors.

Ligand	K_{ic} [μM][a]	K_{iu} [μM][b]	IC_{50} [μM]	Mode of inhibition[c]	Clog*P*[d]
(±)-**7**	0.64±0.1	–	6±0.1	compet.	0.5
8	1.6±0.1	–	19±0.1	compet.	−0.4
9	3.7±0.5	23.5±7.1	79±5.2	mixed	1.5
10	4.2±0.6	21.6±6.2	398±5.1	mixed	1.4
(±)-**11**	32.3±2.8		71±0.1	compet.	0.4
(±)-**12**	0.29±0.1	–	8±0.1	compet.	0.3
(±)-**13**	0.36±0.1	–	6±0.1	compet.	1.3
(±)-**14**	1.2±0.3	–	8±0.2	compet.	2.1
(±)-**15**	2.6±0.1	–	22±1	compet.	−0.03
(±)-**16**	8.2±1.7	27.3±11.1	48±17	mixed	1.0
(±)-**17**	16.3±1.0	–	102±15	compet.	1.9
18	–	–	–	[e]	1.2

[a] K_{ic} = competitive inhibition constant. [b] K_{iu} = uncompetitive inhibition constant. [c] Compet.: competitive inhibition; mixed: mixed competitive - uncompetitive inhibition. [d] The logarithmic partition coefficients Clog*P* were calculated with the program ACD/Log*P* (ACD-Labs) with an uncertainty of ±0.7 to 0.9. [e] 54% Inhibition at [**18**] = 500 μM. [f] Errors for the K_i values were estimated by the program Dynafit; for the IC_{50} values the average was calculated from duplicate measurements and the error given as standard deviation.

best ligands ((±)-**7**, (±)-**12**, and (±)-**13**) in the upper nanomolar range. Binding of the best ligands follows a fully competitive mechanism, whereas for some other derivatives a mixed competitive (K_{ic}) - uncompetitive (K_{iu}) mode of inhibition is observed. Much weaker binding occurs when the ligand lacks the sulfonamide moiety as in the propargylic alcohol derivative **18**. The calculated logarithmic partition coefficients are on the lower side; they nevertheless demonstrate that specific binding rather than more favorable partitioning leads to enhanced activities. Thus the tetrahydrothiophenyl derivatives (±)-**7** with an ethyl (Clog*P* = 0.5, K_{ic} = 0.64 μM) or (±)-**12** with a cyclopropyl (Clog*P* = 0.3, K_{ic} = 0.29 μM) side chain are much better binders than the phenyl derivative (±)-**17** (Clog*P* = 1.9, K_{ic} = 16.3 μM).

The high affinities of the best ligands in the series, together with the kinetic results, generally support the binding mode at the active site of IspE proposed by computer modeling (Figure 3). We note that the tetrahydrothiophenyl ring directly attached to N1 of the cytosine scaffold (as in (±)-**7**, K_{ic} = 0.64 μM) is superior to the ribose substitutes that are attached to N1 by a methylene spacer (as in (±)-**11**, K_{ic} = 32.3 μM). According to modeling, the S-atom of the tetrahydrothiophenyl derivatives (in both enantiomers) can undergo favorable *S*-aromatic interactions of the latter with the neighboring phenolic side chain of Tyr25.[16]

With the tetrahydrothiophenyl substituent at N1 of cytosine kept constant, the substituent at the sulfonamide was systematically varied to explore its optimal size for filling of the small hydrophobic subpocket lined by Leu15, Leu28, and Phe185 (Figure 3). The inhibition constants K_{ic} were found to increase in the sequence cyclopropyl ((±)-**12**) < 2,2,2-trifluoroethyl ((±)-**13**) < trifluoromethyl ((±)-**14**) < methyl ((±)-**15**) < *n*-propyl ((±)-**16**) < phenyl ((±)-**17**) (Table 1)). The binding free enthalpy changes from $\Delta G_{300K} = -9.0$ kcal mol^{-1} for the complex of (±)-**12** to $\Delta G_{300K} = -6.6$ kcal mol^{-1} for the complex of (±)-**17**. The cyclopropyl- and 2,2,2-trifloromethyl-substituted ligands (±)-**12** and (±)-**13** are the best as these residues allow an optimal filling of the small subpocket. The trifluoromethyl and methyl substituted ligands (±)-**14** and (±)-**15** are weaker binders as these residues are too small to fill the pocket. The propyl residue in (±)-**16** can still be incorporated in the pocket, but at the cost of adopting a gauche conformation, which reduces the measured binding affinity.

According to modeling, the phenyl residue in (±)-**17** is too large to occupy this pocket. Although the binding affinity of (±)-**17** is strongly reduced in comparison to that of the best ligands, the K_{ic} value is still in the lower micromolar range. One explanation could be that the residues lining the shallow pocket can reorient to create the space necessary for the accommodation of the phenyl ring. We very much prefer, however, to propose an alternative, strain-free binding geometry of (±)-**17**, in which the favorable conformation of the aryl sulfonamide[7] is maintained, with the phenyl ring directed in the opposite direction away from the hydrophobic pocket and towards the solvent channel (Figure 5). Ultimately, X-ray crystallography of the protein–ligand complexes should provide a definitive answer about the orientation of the sulfonamide side chain.

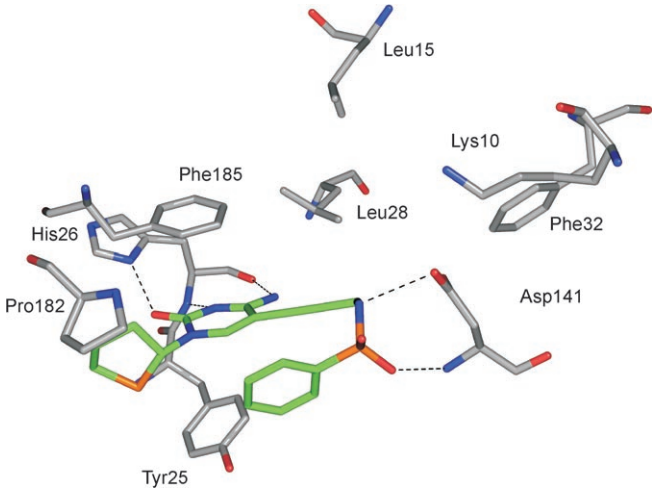

Figure 5. Modeled binding of inhibitor (*R*)-**17** in the active site of IspE. The (*S*)-enantiomer should bind in a similar geometry. As the phenyl residue of (±)-**17** is too large to occupy the small hydrophobic pocket lined by Leu15, Leu28, and Phe185, we propose that it turns in the opposite direction towards the open solvent channel. This orientation does not generate any repulsive contacts and should be quite favorable as the arylsulfonamide maintains its favorable conformation, that is, the N-lone pair and the *p*-orbital on the aromatic *ipso*-C-atom both bisect the O-S-O angle.[7] This preferred conformation was fixed in the modeling.

In summary, we have reported the synthesis and biological evaluation of the first inhibitors of IspE. They are among the first examples of nonphosphate- and nonphosphonate-based inhibitors for the enzymes of the non-mevalonate pathway. In addition, we describe a rare case, in which a kinase inhibitor was designed to occupy the substrate and not the ATP binding

site. This should confer a higher degree of selectivity to our inhibitors. Structure–activity relationships suggest that filling the small hydrophobic pocket lined by Leu 15, Leu 28, and Phe 185, which is not used by the substrate, with appropriately-sized residues leads to a measurable gain in binding free enthalpy. These results mark an important achievement towards synthesizing antimalarials and antimicrobials with a new and innovative mode of action. Further optimization of the ligands, both with respect to affinity and selectivity as well as physicochemical properties, is now underway.

Acknowledgements

*This research was supported by the ETH Research Council and by a graduate student fellowship from the Roche Research Foundation (to A.K.H.H) and by NIH grant R21 NS053634-01 (to A.B., F.R., and W.E). We thank Lukas Brändli for providing compound **38** used as an intermediate in the synthesis of inhibitor **8**.*

Keywords: anti-infective agents · drug design · inhibitors · kinase · non-mevalonate pathway

[1] a) M. Rohmer, M. Knani, P. Simonin, B. Sutter, H. Sahm, *Biochem. J.* **1993**, *295*, 517–524; b) S. T. J. Broers, PhD thesis, ETH Zürich, No. 10978, **1994**; c) M. K. Schwarz, PhD thesis, ETH Zürich, No. 10951, **1994**; d) W. Eisenreich, M. Schwarz, A. Cartayrade, D. Arigoni, M. H. Zenk, A. Bacher, *Chem. Biol.* **1998**, *5*, R221–R233.

[2] a) H. Jomaa, J. Wiesner, S. Sanderbrand, B. Altincicek, C. Weidemeyer, M. Hintz, I. Türbachova, M. Eberl, J. Zeidler, H. K. Lichtenthaler, D. Soldati, E. Beck, *Science* **1999**, *285*, 1573–1576; b) J. Wiesner, R. Ortmann, H. Jomaa, M. Schlitzer, *Angew. Chem.* **2003**, *115*, 5432–5451; *Angew. Chem. Int. Ed.* **2003**, *42*, 5274–5293; c) F. Rohdich, S. Hecht, A. Bacher, W. Eisenreich, *Pure Appl. Chem.* **2003**, *75*, 393–405.

[3] a) B. Greenwood, T. Mutabingwa, *Nature* **2002**, *415*, 670–672; b) R. G. Ridley, *Nature* **2002**, *415*, 686–693; c) A. M. Thayer, *Chem. Eng. News* **2005**, *83*(43), 69–82.

[4] C. M. Crane, J. Kaiser, N. L. Ramsden, S. Lauw, F. Rohdich, W. Eisenreich, W. N. Hunter, A. Bacher, F. Diederich, *Angew. Chem.* **2006**, *118*, 1082–1087; *Angew. Chem. Int. Ed.* **2006**, *45*, 1069–1074.

[5] a) S. Borrmann, S. Issifou, G. Esser, A. A. Adegnika, M. Ramharter, P.-B. Matsiegui, S. Oyakhirome, D. P. Mawili-Mboumba, M. A. Missinou, J. F. J. Kun, H. Jomaa, P. G. Kremsner, *J. Infect. Dis.* **2004**, *190*, 1534–1540; b) T. Haemers, J. Wiesner, R. Busson, H. Jomaa, S. Van Calenbergh, *Eur. J. Org. Chem.* **2006**, 3856–3863; c) V. Devreux, J. Wiesner, J. L. Goeman, J. Van der Eycken, H. Jomaa, S. Van Calenbergh, *J. Med. Chem.* **2006**, *49*, 2656–2660.

[6] For a review on biological phosphate recognition, see: A. K. H. Hirsch, F. R. Fischer, F. Diederich, *Angew. Chem.* **2007**, *119*, 342–357; *Angew. Chem. Int. Ed.* **2007**, *46*, 338–352.

[7] For an illustration of our structure-based design approach for the development of new antimalarials, see: F. Hof, A. Schütz, C. Fäh, S. Meyer, D. Bur, J. Liu, D. E. Goldberg, F. Diederich, *Angew. Chem.* **2006**, *118*, 2193–2196; *Angew. Chem. Int. Ed.* **2006**, *45*, 2138–2141.

[8] a) F. Rohdich, J. Wungsintaweekul, H. Lüttgen, M. Fischer, W. Eisenreich, C. A. Schuhr, M. Fellermeier, N. Schramek, M. H. Zenk, A. Bacher, *Proc. Natl. Acad. Sci. U.S.A.* **2000**, *97*, 8251–8256; b) H. Lüttgen, F. Rohdich, S. Herz, J. Wungsintaweekul, S. Hecht, C. A. Schuhr, M. Fellermeier, S. Sagner, M. H. Zenk, A. Bacher, W. Eisenreich, *Proc. Natl. Acad. Sci. U.S.A.* **2000**, *97*, 1062–1067; c) T. Kuzuyama, M. Takagi, K. Kaneda, H. Watanabe, T. Dairi, H. Seto, *Tetrahedron Lett.* **2000**, *41*, 2925–2928.

[9] a) T. Wada, T. Kuzuyama, S. Satoh, S. Kuramitsu, S. Yokoyama, S. Unzai, J. R. H. Tame, S.-Y. Park, *J. Biol. Chem.* **2003**, *278*, 30022–30027; b) L. Miallau, M. S. Alphey, L. E. Kemp, G. A. Leonard, S. M. McSweeney, S. Hecht, A. Bacher, W. Eisenreich, F. Rohdich, W. N. Hunter, *Proc. Natl. Acad. Sci. U.S.A.* **2003**, *100*, 9173–9178.

[10] a) P. R. Gerber, K. Müller, *J. Comput.-Aided Mol. Des.* **1995**, *9*, 251–268; b) Gerber Molecular Design (http://www.moloc.ch).

[11] a) The conformational restriction of sulfonamides, as evidenced by a search of the Cambridge Structural Database (CSD) was first brought to our attention in the course of a seminar series by Prof. K. Müller (Roche) at ETH Zurich in 2004; b) For analogous conformational preferences of arylsulfones, see [7]; c) Benzenesulfonamide slightly prefers the "eclipsed" over the "staggered" conformation, with the N-lone pair synperiplanar to the S–C bond; V. Petrov, V. Petrova, G. V. Girichev, H. Oberhammer, N. I. Giricheva, S. Ivanov, *J. Org. Chem.* **2006**, *71*, 2952–2956; d) Calculations have shown that in the case of mono- or di-*N*-substituted benzenesulfonamides, the staggered conformation is equally or more favorable, respectively; F. Hof, F. Diederich, unpublished results.

[12] K. A. Watanabe, T.-L. Su, R. S. Klein, C. K. Chu, A. Matsuda, M. W. Chun, C. Lopez, J. J. Fox, *J. Med. Chem.* **1983**, *26*, 152–156.

[13] I. A. O'Neil, K. M. Hamilton, *Synlett* **1992**, 791–792.

[14] V. Illarionova, J. Kaiser, E. Ostrozhenkova, A. Bacher, M. Fischer, W. Eisenreich, F. Rohdich, *J. Org. Chem.* **2006**, *71*, 8824–8834.

[15] P. Kuzmic, *Anal. Biochem.* **1996**, *237*, 260–273.

[16] E. A. Meyer, R. K. Castellano, F. Diederich, *Angew. Chem.* **2003**, *115*, 1244–1287; *Angew. Chem. Int. Ed.* **2003**, *42*, 1210–1250.

Received: January 17, 2007
Published online on March 16, 2007

